INTERNATIONAL JOURNAL FOR NUMERICAL METHODS IN FLUIDS
Int. J. Numer. Meth. Fluids 2008; **56**:965–978
Published online 23 August 2007 in Wiley InterScience (www.interscience.wiley.com). DOI: 10.1002/fld.1583

Fluid–structure interaction problems in free surface flows: Application to boat dynamics

L. Formaggia[1,*,†], E. Miglio[1], A. Mola[1] and N. Parolini[2]

[1]*MOX, Mathematics Department 'F. Brioschi', Politecnico di Milano, Via Bonardi 9, 20133, Milano, Italy*
[2]*CMCS/IACS, Ecole Polytechnique Fédérale de Lausanne, Station 8, CH-1015, Lausanne, Switzerland*

SUMMARY

In this paper, we present some recent studies on fluid–structure interaction problems in the presence of free surface flow. We consider the dynamics of boats simulated as rigid bodies. Several hydrodynamic models are presented, ranging from full Reynolds averaged Navier–Stokes equations to reduced models based on potential flow theory. Copyright © 2007 John Wiley & Sons, Ltd.

Received 24 March 2007; Revised 22 June 2007; Accepted 2 July 2007

KEY WORDS: computational fluid dynamics; fluid–structure interaction; dynamics of rowing

1. INTRODUCTION

The use of computational fluid dynamics (CFD) in boat design is traditionally based on the potential flow theory, although in the last years the use of Reynolds averaged Navier–Stokes (RANS) codes has become increasingly more common. The role of CFD is of particular importance whenever performance optimization is critical, such as in competition boat, where even a small advantage may be crucial. An overview on the numerical techniques for ship hydrodynamics may be found in [1, 2] and, more specifically, their relevance for high performance sailing boat in [3].

In this field, most of the numerical investigations aim to assess the boat characteristics at a given fixed configuration. Furthermore, they usually compute a steady-state solution, even if sometimes this is reached through pseudo-time-stepping. Yet, simulating the full dynamics of a boat may be of great importance [4, 5]. We mention two cases: high-performance sailing boats and rowing sculls. In the former, the accurate simulation of the dynamics may allow for a better trimming of the boat [4, 6], better evaluating wave resistance [7] and in perspective the assessment of its performance during manoeuvring. For a competition rowing scull, accounting for the dynamics

*Correspondence to: L. Formaggia, MOX, Mathematics Department 'F. Brioschi', Politecnico di Milano, Via Bonardi 9, 20133, Milano, Italy.
†E-mail: luca.formaggia@polimi.it

Copyright © 2007 John Wiley & Sons, Ltd.

effects is even more important. Indeed, because of the periodic action at the oars and the movement of the oarsmen on the boat, the motions of the scull is very complex and characterized by horizontal accelerations/decelerations, sinking and dipping. These secondary movements generate waves that dissipate part of rowers energy, that could be better spent to move the boat forward.

In this paper, we give an account of our research in this class of problems. We first give a general framework to describe the dynamics of a boat under the action of the hydrodynamic and other external forces, describing also its integration with RANS codes.

Transient computations using RANS models are computationally demanding, while in the design process there is the need of having tools for fast predictions to compare different design configurations. In the case of the rowing scull, the same tools may also be used to study the effect of different oarsmen layouts or rowing styles. We describe a reduced model for the scull dynamics, where the energy dissipation effects induced by the secondary motions are simulated by computing a suitable potential problem for wave radiation. Despite its simplicity, the approach has proved to be highly effective. Finally, we describe an intermediate model based on the solution of quasi-3D Navier–Stokes equations with free surface [8], where the presence of the boat is modelled through an inequality constraint. We show how the method is able to reproduce the general wave patterns of a moving scull.

2. THE MATHEMATICAL MODELS

The simulation of the fluid dynamic field around a moving boat requires to account for different aspects of the physics of the problem: the viscous effects (including those related to the turbulent nature of the flow) as well as the wave generation on the water free surface. In this work, the structural deformations are not considered (since for the problems at hand their impact on the boat dynamics is negligible) and only the rigid body motion of the boat in the six degrees of freedom is modelled.

2.1. The Reynolds averaged Navier–Stokes equations with free surface

The hydrodynamic flow around the boat can be described by the so-called RANS equations. In this approach, the turbulence effects are suitably modelled and enter the equations through an additional eddy viscosity term, avoiding the need for resolving the small scales (in time and space) which characterize turbulent flows. The presence of the free surface is accounted for by using a multiphase model, where the air flow in the vicinity of the boat is also computed.

Since we want to model the boat dynamics, we need to consider the problem defined on a computational domain $\Omega = \Omega(t)$ (and therefore a computational grid) that changes in time. In this situation, the correct frame to cast the problem is the so-called arbitrary Lagrangian Eulerian (ALE) approach [9, 10]. The equations to be solved are

$$\frac{\partial \rho}{\partial t} + (\mathbf{v} - \mathbf{v}_s) \cdot \nabla \rho = 0 \tag{1a}$$

$$\rho \frac{\partial \mathbf{v}}{\partial t} + \rho(\mathbf{v} - \mathbf{v}_s) \cdot \nabla \mathbf{v} + \operatorname{div} \mathbf{T} = \mathbf{f}_b \tag{1b}$$

$$\operatorname{div} \mathbf{v} = 0 \tag{1c}$$

Copyright © 2007 John Wiley & Sons, Ltd.

DOI: 10.1002/fld

where ρ is the fluid density, p and $\mathbf{v}$ are the flow pressure and velocity, $\mathbf{T}=(\mu+\mu_t)(\nabla\mathbf{v}+\nabla^T\mathbf{v})-p\mathbf{I}$ is the Cauchy stress tensor (with μ_t the turbulent viscosity) and $\mathbf{f}_b=\rho\mathbf{g}$ is the forcing term due to gravity. The term $\mathbf{v}_s$ is the domain velocity associated with the domain motion, and the time derivatives are understood to be ALE time derivatives. Density and viscosity are constant on the two subdomains containing air and water, respectively.

The boundary conditions are usually set by imposing a given velocity profile at the inflow, zero normal stresses at the outflow, symmetry condition on the far-field lateral boundaries and by forcing the velocity of the fluid to be equal to the velocity of the boat at the boat surface.

For the turbulence, we adopt the k–ε model [11] which requires the solution of two additional equations describing the evolution of the turbulent kinetic energy k and the turbulence dissipation rate ε.

The free-surface dynamics is tracked by using the volume of fluid (VOF) method, where the volume fraction c is used to identify the water ($c=1$) from the air ($c=0$) subdomain. A transport equation for c effectively replaces (1a) and reads

$$\frac{\partial c}{\partial t}+(\mathbf{v}-\mathbf{v}_s)\cdot\nabla c=0$$

so that the variable density and viscosity can be defined based on the local value of c as follows:

$$\rho(\mathbf{x})=c(\mathbf{x})\rho_w+(1-c(\mathbf{x}))\rho_a,\quad \mu(\mathbf{x})=c(\mathbf{x})\mu_w+(1-c(\mathbf{x}))\mu_a$$

where the suffixes w and a identify water and air, respectively. For details about the method, the reader may refer to [12].

For the solution of system (1), a finite volume discretization is adopted. For any cell V of the computational grid, the following equations need to be solved:

$$\frac{\mathrm{d}}{\mathrm{d}t}\int_V\rho(\mathbf{x})\,\mathrm{d}V+\int_{\partial V}\rho(\mathbf{x})(\mathbf{v}-\mathbf{v}_s)\,\mathrm{d}\boldsymbol{\gamma}=0$$

$$\frac{\mathrm{d}}{\mathrm{d}t}\int_V\rho(\mathbf{x})\mathbf{v}\,\mathrm{d}V+\int_{\partial V}\rho(\mathbf{x})\mathbf{v}(\mathbf{v}-\mathbf{v}_s)\,\mathrm{d}\boldsymbol{\gamma}=\int_{\partial V}\mathbf{T}\,\mathrm{d}\boldsymbol{\gamma}+\int_V\mathbf{f}_b\,\mathrm{d}V$$

Similar finite volume discretization can be obtained for the transport equations defining the turbulence model as well as for the volume fraction equation.

2.2. *Modelling the boat rigid motion*

A numerical method able to simulate the boat dynamics in calm water and waves requires the coupling between the fluid solver and a code for the structural dynamics.

Following the approach adopted in [4, 13], we consider two orthogonal Cartesian reference frames: an inertial reference system ($\mathbf{O}$, X, Y, Z), which moves forward with the mean boat speed, and a body-fixed reference system ($\mathbf{X}$, x, y, z), whose origin is the boat centre of mass $\mathbf{X}$, which translates and rotates with the boat. The XY plane in the inertial reference system is parallel to the undisturbed water surface and the Z-axis points upward. The body-fixed x-axis is directed from bow to stern and y is a positive starboard.

The dynamics of the boat in the six degrees of freedom is described by the equations of linear and angular momentum, set in the inertial reference frame, and is given by

$$M\ddot{\mathbf{X}}=\mathbf{F}\tag{2}$$

Copyright © 2007 John Wiley & Sons, Ltd.

DOI: 10.1002/fld

and

$$\mathscr{R}\mathscr{I}\mathscr{R}^{-1}\dot{\mathbf{\Omega}} + \mathbf{\Omega} \times \mathscr{R}\mathscr{I}\mathscr{R}^{-1}\mathbf{\Omega} = \mathbf{M}_G \tag{3}$$

respectively. Here, M is the boat mass, $\ddot{\mathbf{X}}$ is the linear acceleration of the centre of mass, $\mathbf{F}$ is the force acting on the boat, $\dot{\mathbf{\Omega}}$ and $\mathbf{\Omega}$ are the angular acceleration and velocity, respectively. Finally, $\mathbf{M}_G$ is the moment with respect to G acting on the boat, $\mathscr{I}$ is the tensor of inertia of the boat about the body-fixed reference system axes and $\mathscr{R}$ is the transformation matrix between the body fixed and inertial reference systems (see [4] for details).

The forces and moments acting on the boat can be expressed as

$$\mathbf{F} = \mathbf{F}_{\text{Flow}} + M\mathbf{g} + \sum_{i=1}^{m} \mathbf{F}_{e_i}$$

$$\mathbf{M}_G = \mathbf{M}_{\text{Flow}} + \sum_{i=1}^{m} (\mathbf{X}_{e_i} - \mathbf{X}) \times \mathbf{F}_{e_i}$$

where $\mathbf{F}_{\text{Flow}}$ and $\mathbf{M}_{\text{Flow}}$ are the force and angular moment due to the interaction with the flow, $\mathbf{F}_{e_i}$ are external forcing terms (which may model, e.g. the wind force on sails or the inertial and traction forces due to the rowers action) and $\mathbf{X}_{e_i}$ are their application points.

To integrate with respect to the equations of motion time, the second-order ordinary differential equations (2)–(3) are formulated as systems of first order ODEs. If we consider, for example, the linear momentum equation (2), it can be rewritten as

$$M\dot{\mathbf{V}} = \mathbf{F}, \quad \dot{\mathbf{X}} = \mathbf{V}$$

where $\mathbf{V}$ denotes the linear velocity of the centre of mass. This system is solved using an explicit two-step Adam–Bashforth scheme for the velocity

$$\mathbf{V}^{n+1} = \mathbf{V}^n + \frac{\Delta t}{2M}(3\mathbf{F}^n - \mathbf{F}^{n-1})$$

and a Crank–Nicholson scheme for the position of the centre of mass

$$\mathbf{X}^{n+1} = \mathbf{X}^n + \frac{\Delta t}{2}(\mathbf{V}^{n+1} + \mathbf{V}^n)$$

For a convergence analysis of the scheme (as well as for a detailed description of the integration scheme for the angular momentum equation), we refer to [14], where it is shown that second-order accuracy in time is obtained, and that the restriction on time step linked to numerical stability is less demanding than that required to capture the time evolution of this class of problems correctly.

In the fluid–structure interaction (FSI) problem, the equilibrium configurations of the structure depends on the configurations of the fluid and *vice versa*. In the coupling with the flow solver, the 6-DOF dynamical system receives at each time step the values of the forces and moments acting on the boat and returns the values of the new position as well as linear and angular velocities. In the flow solver, these data are used to update the computational grid (by a mesh motion strategy based on elastic analogy) and the flow equations (1) in ALE form are solved in the new domain.

2.3. The dynamics of a rowing boat

We now specialize the model for the case of a rowing boat. Due to the presence of rowers exerting on the hull intermittent traction and inertial forces, the main surging motion of a rowing boat is

Copyright © 2007 John Wiley & Sons, Ltd.

DOI: 10.1002/fld

inevitably associated with some secondary motions. The latter causes a consistent additional drag component, mainly by wave radiation and must therefore be considered to get accurate performance predictions.

Equations (2) and (3) in the case of a rowing boat driven by n rowers may be summarized as

$$M\ddot{\mathbf{X}} = \sum_{j=1}^{n} \mathbf{F}_{\mathrm{o}_j} + \sum_{j=1}^{n} \mathbf{F}_{\mathrm{s}_j} + \sum_{j=1}^{n} \mathbf{F}_{\mathrm{f}_j} + M\mathbf{g} + \mathbf{F}_{\mathrm{Flow}} \tag{4a}$$

$$\mathscr{R}\mathscr{I}\mathscr{R}^{-1}\dot{\mathbf{\Omega}} + \mathbf{\Omega} \times \mathscr{R}\mathscr{I}\mathscr{R}^{-1}\mathbf{\Omega} = \sum_{j=1}^{n} (\mathbf{X}_{\mathrm{o}_j} - \mathbf{X}) \times \mathbf{F}_{\mathrm{o}_j} + \sum_{j=1}^{n} (\mathbf{X}_{\mathrm{s}_j} - \mathbf{X}) \times \mathbf{F}_{\mathrm{s}_j} + \sum_{j=1}^{n} (\mathbf{X}_{\mathrm{f}_j} - \mathbf{X}) \times \mathbf{F}_{\mathrm{f}_j} + \mathbf{M}_{\mathrm{Flow}} \tag{4b}$$

where the angular momentum is computed around the hull barycentre. Here, $\mathbf{F}_{\mathrm{o}_j}$, $\mathbf{F}_{\mathrm{s}_j}$, $\mathbf{F}_{\mathrm{f}_j}$ indicate the external forces exerted by each rower on oarlocks, seats and footboards, respectively. They can be obtained by the equations governing the dynamics of the rowers, as it follows.

We represent the mass distribution of an athlete of given characteristics (weight, height, sex) by subdividing the body into p parts, of which we infer the mass m_{ij} from anatomical tables. We then write the momentum equations for the jth rower as

$$\sum_{i=1}^{p} m_{ij}(\ddot{\mathbf{X}}_{ij} - \mathbf{g}) = \mathbf{F}_{\mathrm{h}_j} + \mathbf{F}_{\mathrm{s}_j} + \mathbf{F}_{\mathrm{f}_j} \tag{5a}$$

$$\sum_{i=1}^{p} m_{ij}(\mathbf{X}_{ij} - \mathbf{X}_{\mathrm{f}_j}) \times (\ddot{\mathbf{X}}_{ij} - \mathbf{g}) = (\mathbf{X}_{\mathrm{h}_j} - \mathbf{X}_{\mathrm{f}_j}) \times \mathbf{F}_{\mathrm{h}_j} + (\mathbf{X}_{\mathrm{s}_j} - \mathbf{X}_{\mathrm{f}_j}) \times \mathbf{F}_{\mathrm{s}_j} \tag{5b}$$

Here, $\mathbf{F}_{\mathrm{h}_j}$ is the force at the hand of the jth athlete, whereas $\mathbf{X}_{\mathrm{h}_j}$, $\mathbf{X}_{\mathrm{s}_j}$ and $\mathbf{X}_{\mathrm{f}_j}$ are the positions of the hand, seat and footboard, respectively. $\mathbf{X}_{ij}$ and $\ddot{\mathbf{X}}_{ij}$ indicate the position and acceleration of the barycentre of the ith body part of the jth rower, in the global reference frame. In Equation (5b), we have neglected the contribution to the angular momentum due to each mass rotation around its own centre of mass.

Introducing the values of $\mathbf{F}_{\mathrm{f}}$ and $\mathbf{F}_{\mathrm{s}}$ obtained from (5a) and (5b) into (4a) and (4b), we obtain

$$M(\ddot{\mathbf{X}} - \mathbf{g}) = \sum_{j=1}^{n} \mathbf{F}_{\mathrm{o}_j} + \sum_{j=1}^{n} \mathbf{F}_{\mathrm{h}_j} - \sum_{j=1}^{n} \sum_{i=1}^{p} m_{ij}(\ddot{\mathbf{X}}_{ij} - \mathbf{g}) + \mathbf{F}_{\mathrm{Flow}} \tag{6a}$$

$$\mathscr{R}\mathscr{I}\mathscr{R}^{-1}\dot{\mathbf{\Omega}} + \mathbf{\Omega} \times \mathscr{R}\mathscr{I}\mathscr{R}^{-1}\mathbf{\Omega} = \sum_{j=1}^{n} (\mathbf{X}_{\mathrm{o}_j} - \mathbf{X}) \times \mathbf{F}_{\mathrm{o}_j} + \sum_{j=1}^{n} (\mathbf{X}_{\mathrm{h}_j} - \mathbf{X}) \times \mathbf{F}_{\mathrm{h}_j} - \sum_{j=1}^{n} \sum_{i=1}^{p} (\mathbf{X}_{ij} - \mathbf{X}) \times m_{ij}(\ddot{\mathbf{X}}_{ij} - \mathbf{g}) + \mathbf{M}_{\mathrm{Flow}} \tag{6b}$$

We now assume that the motion of the boat lies in its symmetry plane (i.e. only surge, heave and pitch motions are considered). This approximation is indeed valid for sculls, where each rower acts synchronously on both oars and we can reasonably assume that experienced rowers would

Copyright © 2007 John Wiley & Sons, Ltd.

DOI: 10.1002/fld

minimize movements out of the symmetry plane. Indicating points in the relative reference frame with lower case letters we may write relations

$$\mathbf{X}_{ij} = \mathbf{X} + \mathscr{R}(\phi)\mathbf{x}_{ij} \tag{7a}$$

$$\ddot{\mathbf{X}}_{ij} = \ddot{\mathbf{X}} + \mathscr{R}(\phi)\ddot{\mathbf{x}}_{ij} + 2\dot{\phi}\mathscr{O}(\phi)\dot{\mathbf{x}}_{ij} + \ddot{\phi}\mathscr{O}(\phi)\mathbf{x}_{ij} - \dot{\phi}^2\mathscr{R}(\boldsymbol{\phi})\mathbf{x}_{ij} \tag{7b}$$

to link positions, velocities and accelerations in the two reference frames. Here, ϕ is the angle of rotation w.r.t. the y-axis, while $\mathscr{R}$ and $\mathscr{O}$ are 2×2 rotation matrices, namely

$$\mathscr{R} = \begin{bmatrix} \cos\phi & -\sin\phi \\ \sin\phi & \cos\phi \end{bmatrix}, \quad \mathscr{O} = \begin{bmatrix} -\sin\phi & -\cos\phi \\ \cos\phi & -\sin\phi \end{bmatrix}$$

Substituting Equations (7) in Equations (6), we have finally that

$$\left(M + \sum_{i,j} m_{ij}\right)\ddot{\mathbf{X}} + \mathscr{O}\left(\sum_{i,j} m_{ij}\mathbf{x}_{ij}\right)\ddot{\phi} = -\mathscr{R}\sum_{j,j} m_{ij}\ddot{\mathbf{x}}_{ij} - 2\mathscr{O}\left(\sum_{i,j} m_{ij}\dot{\mathbf{x}}_{ij}\right)\dot{\phi}$$
$$+ \mathscr{R}\left(\sum_{i,j} m_{ij}\mathbf{x}_{ij}\right)\dot{\phi}^2 + \sum_{j=1}^{n}\mathbf{F}_{\mathrm{o}_j} + \sum_{j=1}^{n}\mathbf{F}_{\mathrm{h}_j} + \left(M + \sum_{i,j} m_{ij}\right)\mathbf{g} + \mathbf{F}_{\mathrm{Flow}} \tag{8a}$$

and

$$\mathscr{R}\left(\sum_{i,j} m_{ij}\mathbf{x}_{ij}\right) \times \ddot{\mathbf{X}} + \left(I_{YY} + \sum_{i,j} m_{ij}|\mathbf{x}_{ij}|^2\right)\ddot{\phi}$$
$$= -\mathscr{R}\sum_{i,j} m_{ij}\mathbf{x}_{ij} \times \mathscr{R}\ddot{\mathbf{x}}_{ij} - 2\left(\sum_{i,j} m_{ij}\mathscr{R}\mathbf{x}_{ij} \times \mathscr{O}\dot{\mathbf{x}}_{ij}\right)\dot{\phi} + \sum_{i,j} m_{ij}$$
$$+ \mathscr{R}\sum_{j=1}^{n}\mathbf{x}_{\mathrm{s}_j} \times \mathbf{F}_{\mathrm{s}_j} + \mathscr{R}\sum_{j=1}^{n}\mathbf{x}_{m_j} \times \mathbf{F}_{m_j}\mathscr{R}\sum_{i,j} m_{ij}\mathbf{x}_{ij} \times \mathbf{g} + \mathbf{M}_{\mathrm{Flow}} \tag{8b}$$

where in $\sum_{i,j}$ the indexes i and j run from 1 to p and 1 to n, respectively. Values for oarlock and hand forces (respectively $\mathbf{F}_{\mathrm{o}_j}$ and $\mathbf{F}_{\mathrm{h}_j}$) are provided by measurements on rowing machines, while the motion laws $\mathbf{x}_{ij}(t)$ for the rower body parts are measured using the motion capture techniques [15].

Hence, Equations (8) are a system of three nonlinear second-order ODEs in the variables ($\mathbf{X}$, ϕ) that must be complemented by a suitable fluid dynamic model in order to compute $\mathbf{F}_{\mathrm{Flow}}$ and M_{Flow} and close the problem, for instance, the RANS model presented.

3. REDUCED MODELS FOR THE FSI PROBLEM

An alternative to RANS simulations is to use simplified models to reduce the computational cost, while maintaining an acceptable accuracy.

Copyright © 2007 John Wiley & Sons, Ltd.

DOI: 10.1002/fld

3.1. Potential model for the calculation of the effects of secondary motions

In the first reduced model we present, forces and moments exerted on the hull by the surrounding fluid ($\mathbf{F}_{\text{Flow}}$ and M_{Flow} in Equation (9)) are decomposed as follows:

$$\mathbf{F}_{\text{Flow}} = L_S \mathbf{e}_Z - D_S \mathbf{e}_X + \mathbf{F}_D, \quad M_{\text{Flow}} = M_S + M_D \tag{9}$$

Here, L_S and M_S are the hydrostatic lift and moment which can be readily approximated from the instantaneous position of the hull. The total drag due to the primary surging motion D_S is computed using the formula

$$D_S = \tfrac{1}{2}\rho S_{\text{Ref}} C_{dX} (\dot{G}_X)^2$$

where S_{Ref} is the wet surface, which again depends on the instantaneous position of the boat, and C_{dX} a drag coefficient, estimated for each boat by performing one (or more) Navier–Stokes simulations of the stationary motion.

The forces and moments due to the secondary motions of the boat, here indicated by $\mathbf{F}_D$ and M_D, respectively, are computed by solving, in the computational domain Ω depicted in Figure 1, the following Laplace problem [16] for the complex velocity potential ψ_α:

$$\begin{aligned}
\Delta\psi_\alpha &= 0 \quad \text{on } \Omega \\
\frac{\partial\psi_\alpha}{\partial z} - \frac{\omega^2}{g}\psi_\alpha &= 0 \quad \text{on } \Gamma_{fs} \\
\frac{\partial\psi_\alpha}{\partial n} - \mathrm{i}\frac{\omega^2}{g}\psi_\alpha &= 0 \quad \text{on } \Gamma_\infty \ , \quad \alpha = 1, 2, 3 \\
\frac{\partial\psi_\alpha}{\partial n} &= 0 \quad \text{on } \Gamma_b \\
\frac{\partial\psi_\alpha}{\partial n} &= N_\alpha \quad \text{on } \Gamma_c
\end{aligned} \tag{10}$$

From a physical point of view, it corresponds to solve three problems where a periodic motion of frequency $f = \omega/2\pi$ in the direction of the three degrees of freedom considered is imposed to the boat surface. The non-homogeneous Neumann conditions applied on the boat surface for each problem are therefore the components of the generalized normal vector $N = (n_x, n_z, zn_x - xn_z)$, (n_x, n_y, n_z) being the normal to the boat surface. A few simplifications were necessary to obtain the potential problem. In particular, a linearized form of the free surface interface conditions has been adopted and the equations are in fact solved in the reference configuration.

The forces due to secondary motions are finally computed by integrating the pressure on the boat surface. It turns out that these forces present a component proportional to the acceleration vector $(\ddot{\mathbf{X}}, \ddot{\phi})$, giving rise to an added mass matrix $\mathscr{M}$, and a component proportional to the velocity vector $(\dot{\mathbf{X}}, \dot{\phi})$, leading to a damping matrix $\mathscr{S}$. As for the angular velocity ω, we have taken the one which corresponds to the principal frequency of the motion of the rowers.

3.2. Models based on variational inequalities

Another possibility is to enforce the presence of a floating body in the context of the quasi-3D shallow water formulation described in [8]. To illustrate the technique, we consider a simplified

Copyright © 2007 John Wiley & Sons, Ltd.

DOI: 10.1002/fld

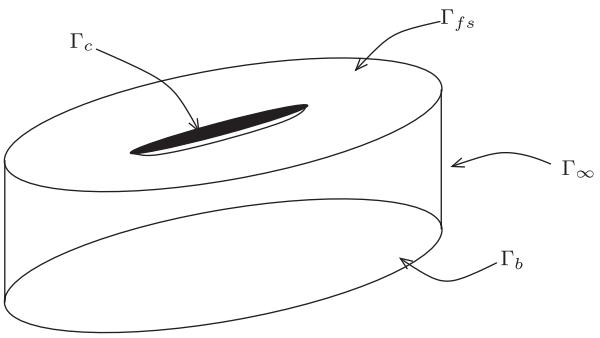

Figure 1. The computational domain for the potential problem (10).

system based on the hydrostatic approximation. This approximation reduces the vertical momentum equation to the static relation $\partial p/\partial z = -\rho g$. We also assume that the position of the free surface η can be described by a single-valued function of x and y, i.e. $\eta = \eta(x, y, t)$ and that the water domain is given by $\Omega = \Omega_{2D} \times (-h, \eta)$, h being the quota of the water bottom (here taken constant) and Ω_{2D} a two-dimensional domain.

Under these hypotheses, the motion of the fluid can be described by the following system of equations:

$$\begin{aligned} \frac{\partial \mathbf{u}}{\partial t} + (\mathbf{v} \cdot \nabla_{xy})\mathbf{u} - \operatorname{div} \boldsymbol{\sigma}_{xy} + g\nabla_{xy}\eta &= -\nabla_{xy}\left(\frac{p_s}{\rho}\right) \\ \frac{\partial \eta}{\partial t} + \operatorname{div} \int_{-h}^{\eta} \mathbf{u}\, \mathrm{d}z &= 0 \\ \operatorname{div} \mathbf{u} + \frac{\partial w}{\partial z} &= 0 \end{aligned} \tag{11}$$

where the unknowns are the horizontal components of the velocity $\mathbf{u} = (v_x, v_y)$, the vertical component $w = v_z$ and the elevation η. Here, ∇_{xy} is the nabla operator in the (x, y) plane, $\boldsymbol{\sigma}_{xy}$ contains the viscous contribution to the first two rows of the Cauchy stress tensor $\mathbf{T}$ and $p_s = p_s(x, y, t)$ is a pressure pattern acting on the free surface.

The idea to account for the boat presence is to reformulate the problem as a constrained one. We assume that the position of the external surface of the boat at each time t can be described by a single-valued function $\Psi = \Psi(x, y, t)$, suitably extended to cover all Ω_{2D}. The constraint then reads, for all t,

$$\eta \leqslant \Psi \quad \text{in } \Omega_{2D} \tag{12}$$

where the equality applies in the region where the free surface is in contact with the body. To enforce the previous inequality, we introduce a Lagrange multiplier $\lambda = \lambda(x, y, t)$. By inspection, it can be found that λ can be interpreted as a perturbation to the pressure applied to the surface, that is, we may write

$$p_s(x, y, t) = p_a + \lambda(x, y, t) \tag{13}$$

Copyright © 2007 John Wiley & Sons, Ltd.

DOI: 10.1002/fld

where p_a is the constant atmospheric pressure (often taken equal to zero). Introducing this last expression into (11) and adding the constraint (12) to the system give rise to a saddle point problem. It is solved by an Uzawa iterative method where the constrained problem is reduced to a sequence of unconstrained problems of the form (11).

When considering the dynamics of the scull, the value of Ψ at each time step is given by solving Equations (8), where the hydrodynamic forces are computed by integrating the surface stress provided by the Navier–Stokes model presented.

From the numerical point of view, problem (11) leads to very efficient computer implementations. For the space discretization, we have adopted a finite element scheme which employs Raviart–Thomas $\mathbb{RT}_0$ triangular elements in the (x, y) plane for $\mathbf{u}$ and standard P^1 elements for w. The elevation η, as well as the multiplier λ, is approximated by a piecewise constant function.

It is also possible to account efficiently for non-hydrostatic effects by a change in the formulation, which we have omitted to illustrate for the sake of space. In any case, the model relies on the assumptions made on the domain shape as well as on the hypothesis that the horizontal components of water velocity are dominant w.r.t. the vertical one. This is not so limitative for rowing boats.

4. RESULTS

4.1. RANS simulations

Several numerical simulations have been carried out to assess the accuracy of the model introduced in Section 2.1. The coupling between the RANS flow solver and the 6-DOF dynamical system was used to predict the ship's running attitude for a Series 60 hull in different sea conditions (see [14]).

Here, we present the results concerning the stabilization behaviour of the hull subjected to a roll forcing moment. We start from a steady symmetric solution and we impose a time-dependent rolling moment given by $M_{x,\text{ext}} = 20\,H(0.5-t)(\sin(2t))^2$, where H is the Heaviside function. Under this external moment, the boat reaches a maximum roll angle of about 15° and then stabilizes to the symmetric equilibrium state. The position of the hull and the free surface around it at different time instants during the stabilization process are reported in Figure 2.

The time evolution of the roll angle for two different values of the moment of inertia around the roll axis is given in Figure 3. As expected, the hull with the smaller moment of inertia reaches a larger maximal roll angle and then stabilizes more quickly. In Table I, we report the

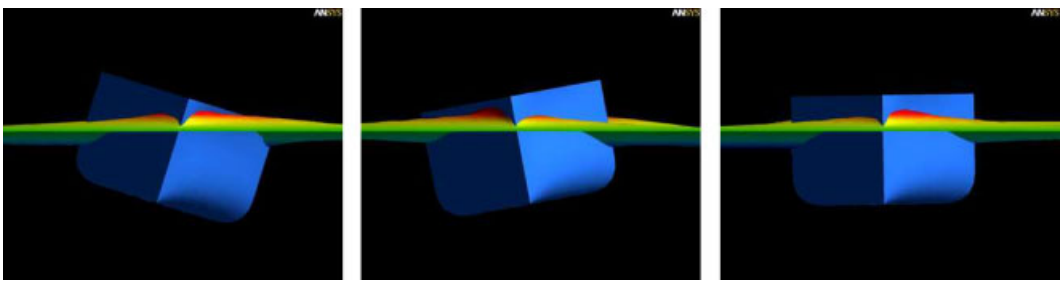

Figure 2. Bow wave around the hull at different time instants during the roll stabilization.

Copyright © 2007 John Wiley & Sons, Ltd.

DOI: 10.1002/fld

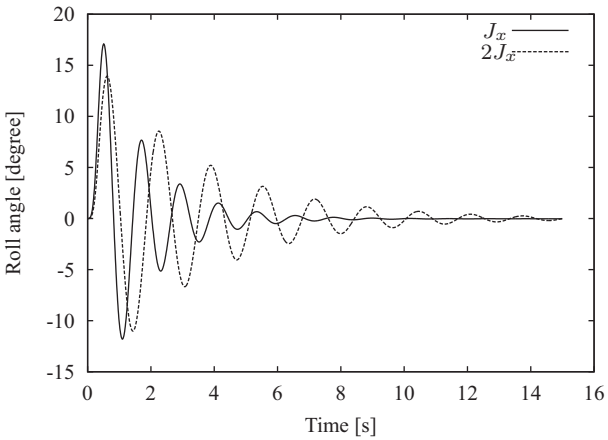

Figure 3. Time evolution of the roll angle with different moments of inertia.

Table I. Damped oscillation parameters for different moments of inertia.

	$A_{\max}$	T (s)	δ
I_{xx}	$0.098L$	1.21	0.8
$2I_{xx}$	$0.080L$	1.64	0.5

maximal amplitude of the roll angle oscillation $A_{\max}$, its period T and the damping factor defined as $\delta = \ln(\phi_j/\phi_{j+1})$ where ϕ_j is the value of the roll angle at the jth maximum. This kind of analysis is very useful in characterizing the dynamic behaviour of a boat.

4.2. Potential model

The fluid dynamic model described in Section 3.1 has been first used to reproduce measurements data available in the literature. In Figure 4, on the left, we report the horizontal velocity time history measured on a single scull driven at 20 strokes per minute. The agreement of the corresponding computed time history (Figure 4, right) appears qualitatively good, although differences between the measured and computed values can be observed in correspondence with the beginning of each stroke. Since no data on the rower were available for these measurements, both his physical characteristics and the inertial and traction forces due to his motion on the boat had to be reconstructed. We believe therefore that this error is mostly due to the difference between the reconstructed dynamics of the rower and the actual dynamics in the considered experiment.

Besides computing the horizontal velocity, our software predicts the complete dynamics of a rowing boat in its symmetry plane, once the boat geometrical data and the physical characteristics and kinematics of the rowers are provided.

A typical output is depicted in Figure 5, which shows the positions and velocities along the X and Z directions, as well as the pitch angle and angular velocity, comparing two configurations with the same scull and rowers of different weights, pushing with a cadence of 40 strokes per minute.

Copyright © 2007 John Wiley & Sons, Ltd.

DOI: 10.1002/fld

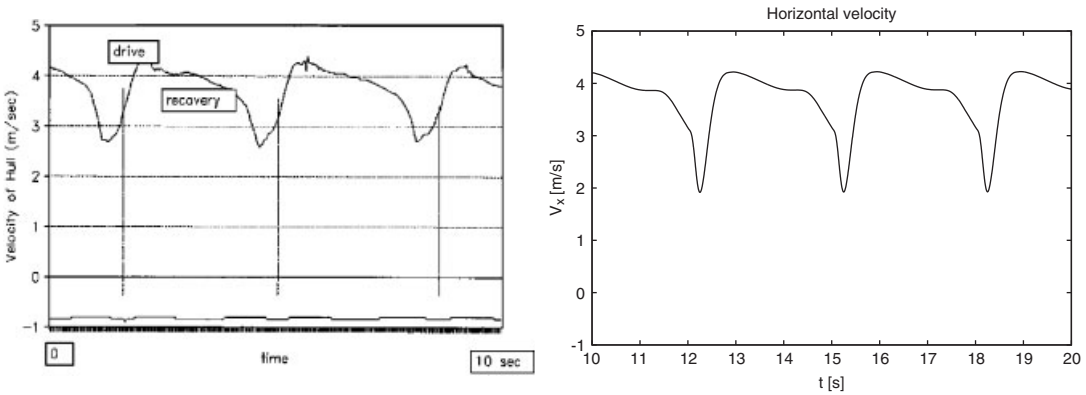

Figure 4. Measured (left) and computed (right) time history of velocity for a single scull. The picture with the experimental velocity data is courtesy of the Department of Physics of the University of Washington.

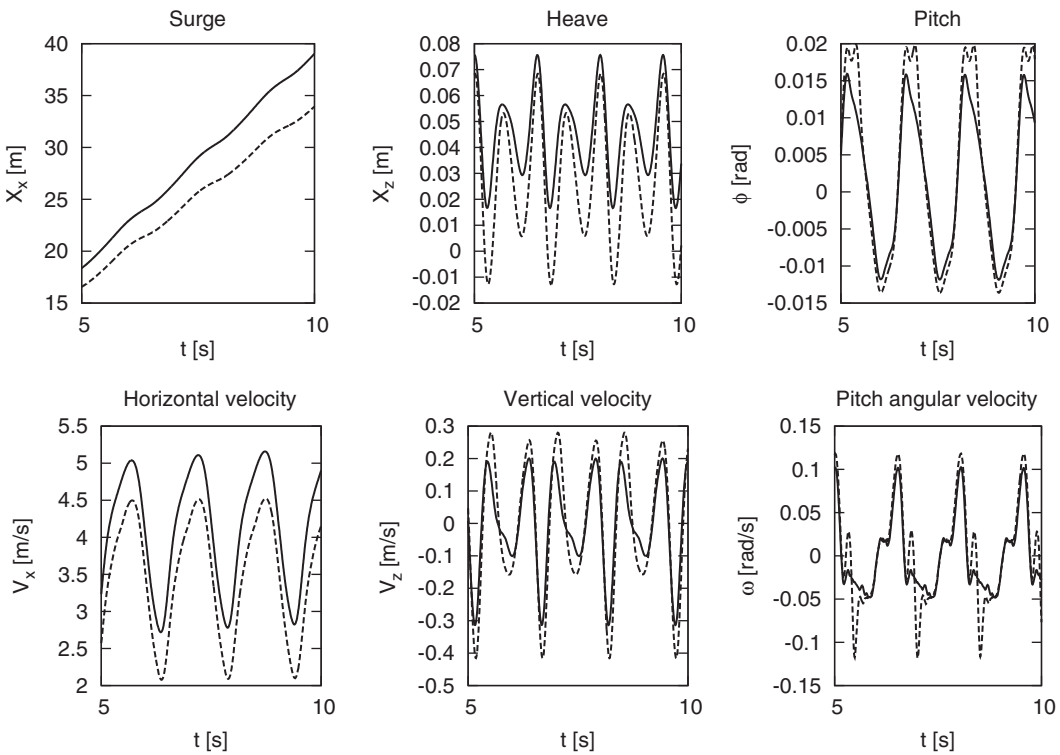

Figure 5. Positions and velocities for a single scull pushed by two different rowers. The first weighting 106 kg (dashed line) and the second 80 kg (continuous line).

Copyright © 2007 John Wiley & Sons, Ltd.

DOI: 10.1002/fld

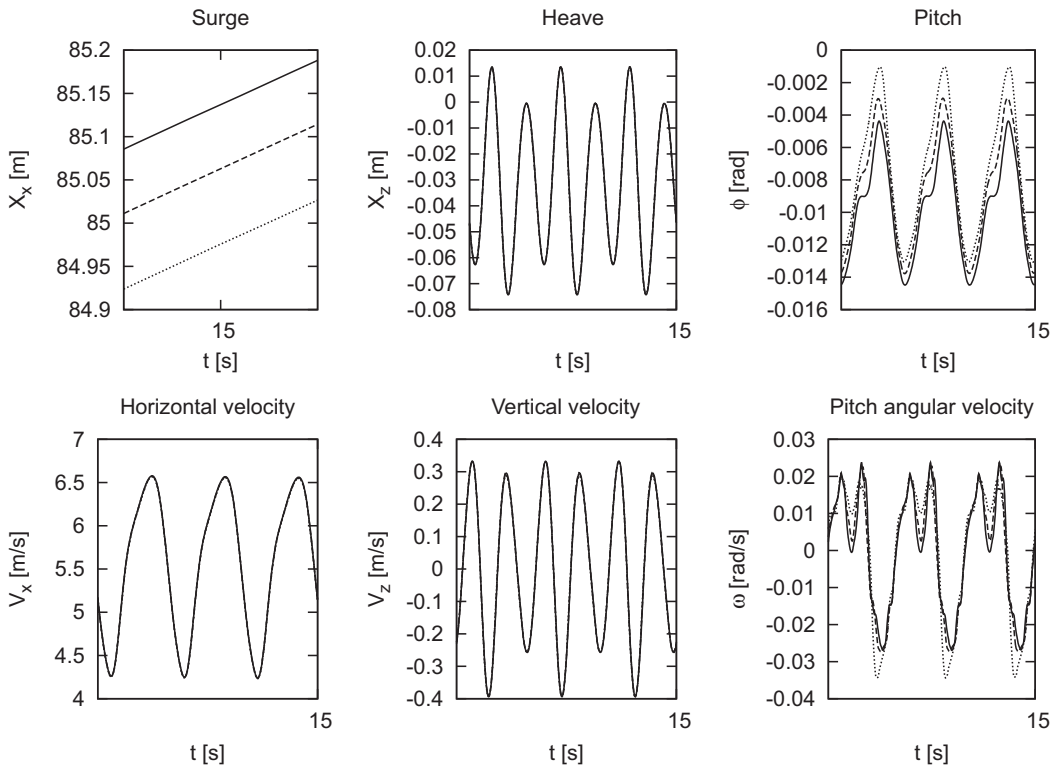

Figure 6. Positions and velocities for a four scull pushed by rowers placed in three different longitudinal positions on the boat. Athletes are moved aft (continuous line) and forward (dotted line) with respect to a reference position (dashed line).

As expected, the heavier rower's boat proceeds with a deeper sinkage, determining a larger wet surface and hence higher drag, which obviously reduces his speed with respect to the lighter rower. To obtain the same performance, he has to change the rowing style and possibly push harder. Being able to assess rapidly the performance changes due to a modification in the rower characteristics makes this model potentially useful also for trainers and athletes.

Finally, we present an example of how the program is employed in the design process of rowing boats. Figure 6 shows the comparison among the predicted performances of a four scull when three different configurations are used. In order to define the optimal longitudinal positioning of the rowers along the boat, the scull performances are tested and compared for three different longitudinal positions of the crew on the boat: starting from a reference position, in one case the rowers are displaced by 10 cm towards the boat bow, while in the other they are moved 10 cm towards the stern. The result shows potential beneficial effects of rowers' displacement in the aft direction. The impact of these differences on the race can be evaluated by considering that for a 2000 m race field the aft position presents an advantage on the other configurations of 2 and 4 m, respectively. It may seem little; however, races are often won for very small differences.

Copyright © 2007 John Wiley & Sons, Ltd.

DOI: 10.1002/fld

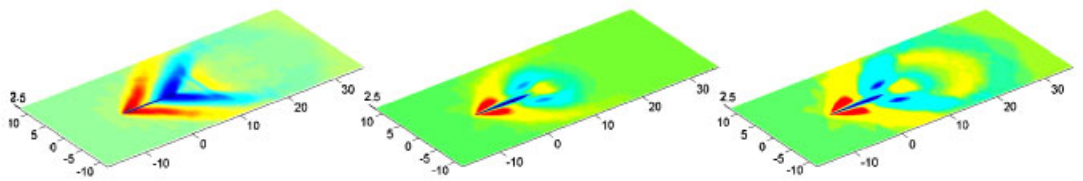

Figure 7. The surface wave pattern for the mean motion (left) and at two different time instants obtained using the full boat dynamics.

4.3. Constraint inequality model

We have considered a coaxless quad scull. The first picture in Figure 7 illustrates the wave pattern generated by the boat moving at a constant mean velocity, computed using the model given in Section 3.2. The second and third pictures illustrate that obtained at the instant of the catch and at the release, when the full dynamics of the boat is considered. We have assumed a stroke period of 1.5 s.

The alteration to the wave pattern caused by the secondary motions is evident. Comparison with experimental data is currently under way. So far, we have carried out only qualitative assessment comparing the wave pattern with that obtained from video recording, with good agreements.

5. CONCLUSIONS

We have illustrated a hierarchy of models recently developed to simulate the dynamics of boats. Each model has its own advantages and limitations. The RANS-based models are in principle capable of capturing the complete physics; yet, they are rather costly, both in terms of the time needed to prepare of a good mesh and in terms of the computational cost of a simulation.

Reduced models are better suited in the preliminary design phase. For the case of scull dynamics, we have presented two possibilities. In the simplest one, the hydrodynamic forces by the mean motion are expressed by simple formula, while the effect of the secondary motions are accounted for by solving a potential problem for wave radiation. This greatly reduces the computational complexity allowing to obtain a result in a matter of minutes. Despite the simplifications made, the model is capable of giving useful indications on the boat performance. For this reason, it has been implemented in a software currently used for preliminary design by a boat manufacturer.

The intermediate model we presented last is in fact still under development. The results obtained so far are, however, very encouraging. It leads to rather efficient algorithms under reasonable assumptions.

A natural further development of this study is the use of these tools for automatic shape optimization.

ACKNOWLEDGEMENTS

The authors wish to thank Filippi Lido s.r.l and in particular Ing. Alessandro Placido for the financial and technical support, and for having introduced them to the world of rowing. The authors also thank Matteo Lombardi and Andrea Paradiso for making some results available from their master theses.

Copyright © 2007 John Wiley & Sons, Ltd.

DOI: 10.1002/fld

REFERENCES

1. Bulgarelli UP, Lugni C, Landrini M. Numerical modelling of free-surface flows in ship hydrodynamics. *International Journal for Numerical Methods in Fluids* 2003; **43**(5):465–481.
2. Bulgarelli UP. The application of numerical methods for the solution of some problems in free-surface hydrodynamics. *Journal of Ship Research* 2005; **49**(4):288–301.
3. Parolini N, Quarteroni A. Mathematical models and numerical simulations for the America's Cup. *Computer Methods in Applied Mechanics and Engineering* 2005; **194**(9–11):1001–1026.
4. Azcueta R. Computation of turbulent free-surface flows around ships and floating bodies. *Ship Technology Research* 2002; **49**(2):46–69.
5. Parolini N, Quarteroni A. Modelling and numerical simulation for yacht design. *Proceedings of the 26th Symposium on Naval Hydrodynamics*, Rome, Italy, 17–22 September 2006, 2007.
6. Yang C, Lohner R. Calculation of ship sinkage and trim using a finite element method and unstructured grids. *International Journal of Computational Fluid Dynamics* 2002; **16**(3):217–227.
7. Orihara H, Miyata H. Evaluation of added resistance in regular incident waves by computational fluid dynamics motion simulation using an overlapping grid system. *Journal of Marine Science and Technology* 2003; **8**(2):47–60.
8. Miglio E, Quarteroni A, Saleri F. Finite element approximation of quasi-3D shallow water equations. *Computer Methods in Applied Mechanics and Engineering* 1999; **174**(3–4):355–369.
9. Donea J. Arbitrary Lagrangian Eulerian methods. *Computational Methods for Transient Analysis*, Computational Methods in Mechanics, vol. 1. North-Holland, Elsevier: Amsterdam, 1983.
10. Formaggia L, Nobile F. A stability analysis for the Arbitrary Lagrangian Eulerian formulation with finite elements. *East-West Journal of Numerical Mathematics* 1999; **7**:105–131.
11. Mohammadi P, Pironneau O. *Analysis of the k–epsilon Model*. Masson: Paris, 1994.
12. Hirt CW, Nichols BD. Volume of fluid (VOF) method for the dynamics of free boundaries. *Journal of Computational Physics* 1981; **39**:201–225.
13. Azcueta R. RANSE simulations for sailing yachts including dynamic sinkage and trim and unsteady motions in waves. *High Performance Yacht Design Conference*, Auckland, 2002; 13–20.
14. Lombardi M. Simulazione numerica della dinamica di uno scafo. *Master Thesis* (in italian), Mathematics Department, Politecnico di Milano, 2006.
15. Mola A, Formaggia L, Miglio E. Simulation of the dynamics of an olympic rowing boat. *Proceedings of ECCOMAS CFD 2006*, Egmond aan Zee, TU Delft, The Netherlands, 5–8 September 2006. ISBN: 90-9020970-0.
16. Mei CC. *The Applied Dynamics of Ocean Surface Waves*. World Scientific: Singapore, second printing with corrections, 1989.

Copyright © 2007 John Wiley & Sons, Ltd.

DOI: 10.1002/fld